



ISSN: 1813-162X (Print); 2312-7589 (Online)

Tikrit Journal of Engineering Sciences

available online at: <http://www.tj-es.com>

TJES

Tikrit Journal of
Engineering Sciences

Underwater Wireless Optical Communication for IOT using Coding MIMO Diversity

Suaad Sabeer Abdulsada *, Mustafa Dh. Hassib , Zainab N. Jameel 

Department of Communication Engineering, University of Technology, Baghdad, Iraq.

Keywords:

UWOC; MIMO; MISO; Concatenated Code; IOU.

Highlights:

- The research paper investigating the relationship between transmitted power and BER for UWOC with and without coding and is combined with MIMO system to overcome the physical layer of IoUT.
- To reduce the error bit in data transmission and underwater attenuation.

ARTICLE INFO

Article history:

Received	29 Mar.	2023
Received in revised form	26 July	2023
Accepted	26 Sep.	2023
Final Proofreading	26 Nov.	2023
Available online	09 June	2024

© THIS IS AN OPEN ACCESS ARTICLE UNDER THE CC BY LICENSE. <http://creativecommons.org/licenses/by/4.0/>



Citation: Abdulsada SS, Hassib MD, Jameel ZN. Underwater Wireless Optical Communication for IOT using Coding MIMO Diversity. *Tikrit Journal of Engineering Sciences* 2024; 31(1): 152-160. <http://doi.org/10.25130/tjes.31.1.13>

*Corresponding author:



Suaad Sabeer Abdulsada

Department of Communication Engineering, University of Technology, Baghdad, Iraq.

Abstract: The present study examined and simulated the coding or no coding performance for different configurations of multi-input, multioutput underwater wireless optical communication systems. MIMO diversity and channel coding were used to reduce the power transmitter, assuming lognormal distribution random for weak ocean turbulence. The simulation tested for a link range of 30 m in low ocean turbulence and 500 Mbps on-off-keying was also presented using Monte-Carlo. The results showed improvement in power transmitted (gain) for 2x5 compared to Uncoded SISO, which was about 33.60db using the concatenated code. So that the underwater wireless optical communications (UWOC) even now will also be significantly impacted by the Internet of Underwater Things (IoUT) and ultimate mobile technologies five generation communication systems because of their extraordinarily high demand for data safety, bit rate, energy consumption, so it is used in combined data transfer between underwater communication devices. The UWOC system based on coded MIMO may successfully be used in IoUT due to its high robustness and power qualification.

الاتصال البصري اللاسلكي تحت الماء لانترنت الأشياء باستخدام تشفير ومتعددات الادخال ومتعدد الاخراج

سعاد صبير عبد السادة، مصطفى ضياء حسيب، زينب ناصر جميل

قسم هندسة الاتصالات / الجامعة التكنولوجية / بغداد – العراق.

الخلاصة

تم فحص ومحاكاة أداء استخدام الترميز أو عدم الترميز لتكوين مختلف لأنظمة الاتصالات الضوئية اللاسلكية تحت الماء متعددة المدخلات والمخرجات. يستخدم تنوع MIMO وتشفير القناة لتقليل مرسل القدرة وافترض التوزيع اللوغاريتمي الطبيعي العشوائي لاضطراب امواج المحيط الضعيف. تم اختبار المحاكاة الخاصة بهذه الدراسة لنطاق الارتباط ٣٠ مترًا في اضطرابات المحيطات المنخفضة و ٥٠٠ ميجا بت في الثانية عند استخدام التضمين نوع on-off، باستخدام مونت كارلو. أظهرت النتائج تحسناً في القدرة المرسل (الكسب) 2×5 عند المقارنة فيما يتعلق ب-SISO غير المشفر، تبلغ حوالي ٣٣,٦٠ ديسيبل عند استخدام الكود المتسلسل. لذا فإن الاتصالات الضوئية اللاسلكية تحت الماء (UWOC) ستؤثر بشكل كبير بانترنت الأشياء تحت الماء (IoUT) بالإضافة إلى تقنيات الهاتف المحمول النهائية لأنظمة الاتصالات من الجيل الخامس نظرًا لطلبها كميات عالية بشكل غير عادي من أمان البيانات ومعدل البيت واستهلاك الطاقة لذلك تم استخدامه في نقل بيانات مجمعة بين أجهزة الاتصالات تحت الماء. يتمتع نظام UWOC القائم على MIMO المشفر بإمكانية استخدامه بنجاح في IoUT نظرًا لقوته العالية وتأهيله للطاقة.

الكلمات الدالة: UWOC، MIMO، MISO، الكود المتسلسل، IoUT.

1. INTRODUCTION

One of the most intriguing technologies that emerged last year is the Internet of Things (IoT), which refers to devices connected to the Internet. IoT advancements aim to connect the entire world and enable computation anywhere. Humans live on a water planet, i.e., 70% of it is covered in water. So, when it is about connecting the entire world, it has not overlooked its bulk. If most of the planet part of the IoT can be made, it will open a whole new universe of data, piquing researchers' curiosity about the Internet of Underwater Things. The Internet of Things was initially introduced in 1985 because of its high cost [1]. Many undersea services, such as ocean monitoring, safe navigation, and disaster prevention, could be enabled by this technology [2]. Beam absorption, dispersion, and underwater turbulence are the main limiting constraints for underwater wireless optical communications (UWOC) systems. Jamali et al. [3] suggested that the sum of lognormal random variables should be approximated using the Gauss-Hermite quadrature formula and the photon-counting technique to assess the system BER. The 3x1 MISO transmission in a 25 m coastal water link with a log amplitude variance of 0.16 increased performance by 8 dB at the BER of 10^{-9} in the presence of shot noise and noted that the MIMO UWOC systems performance significantly suffered from spatial correlation. The order of diversity was reduced by one at a correlation value of $\rho = 0.25$ between the links of a 3x1 MISO UWOC system with $\sigma_x = 0.4$. Due to its scalability, dependability, and flexibility, underwater wireless optical communications (UWOC) have been established to suit various demands in diverse underwater applications. Optical transmission provides a higher bandwidth, better security, and shorter temporal lag than traditional transmission acoustic communication, making UWOC a viable option for high-speed and large-data underwater communications applications, such as photography, real-time video transmission,

and high-throughput sensor networks [4]. Zhu et al. [5] covered sophisticated modulation formats, underwater channels, and system transmitters and receivers. The authors listed some essential UWOC transmission capacity-improving methods. It was concluded that water absorption and scattering characteristics are the primary phenomena that vary the underwater propagation of optical light. Turbulence is the primary cause that fades on optical signals traveling across turbulent seawater in the UWOC systems by providing a closed-form expression for the relationship between temporal correlation, propagation distance, and average velocity for the moving medium's weak turbulence region. The temporal correlation coefficient rises as temperature fluctuation takes over but falls as salinity fluctuation takes over [6]. There is much interest in improving connection performance without increasing transmit power, which is useful for the Internet of Underwater Things applications [2]. A large-area white underwater solid-state lighting system and high-speed underwater wireless optical communication system made of lasers. The system was theoretically illustrated and methodically examined. The outcomes set the stage for future applications in underwater wireless networks and the Internet of Underwater Things [7]. Error correction coding is a sensible solution in this case. Several prior studies have investigated suitable signal modulation techniques for UWOC systems focusing on intensity modulation with direct detection (IM/DD) due to its ease of implementation [8]. The offered coded MIMO techniques can be helpfully employed in constructing UWOC systems to enable IoUT applications, such as inter-submarine communication, submarine-to-port communication, and communication between sensors collecting oceanic parameters and aggregating devices [9]. Also, a 15-m water channel can be used for error-free picture

transmission using the reed Solomon code (RS) coding, discrete Fourier transform spread, discrete multi-tone (DFT-S), and diversity reception techniques. Because of its portability and low power requirements, the proposed UWOC system has a promising future in underwater applications over short to moderate distances [10]. The structure of this paper is divided into five parts. The first part included an On-Off Keying (OOK) modulation in terms of bit error rate (BER). Oriented UWOC systems in weak turbulence and propagation loss due to beam attenuation zones examined different configurations of multi-input, multioutput (MIMO) first with no code and second using a concatenated code reed Solomon and convolution code. The term "improvement" through this study refers to the transmit power decrease observed to achieve a BER of 10^{-5} . The second part explains the characteristics and factors affecting the UWOC. The system model and channel are cleared in part three. Monte-Carlo simulation provided results of the BER as a function of transmit

power in part four, and the conclusions are listed in part five.

2. UNDERWATER CHARACTERISTICS AND FACTORS AFFECTING UWOC

When used as wireless communication carriers, the range of optical waves is usually quite small. This restriction is necessary because of the strong backscatter from particles and the substantial water absorption in the optical frequency band. Optical signals are notoriously attenuated by water, and all particles in the ocean are optically dispersed; thus, resolving either of these issues is a substantial challenge. However, ocean water has lower absorption in the blue/green region of the visible spectrum. For illustration, in the blue/green zone, a high-speed link can be established using the appropriate wavelength for the water's clarity (400-500) nm for clear water to (300-700) nm for muddy water situations). Attenuation is at its lowest at 0.460m in transparent waters and at its highest near 0.540m in murky waters at mid-ocean, as shown in Fig. 1 [11, 12]; also, Table 5 shows the range of the optical wavelength for different types of water [4].

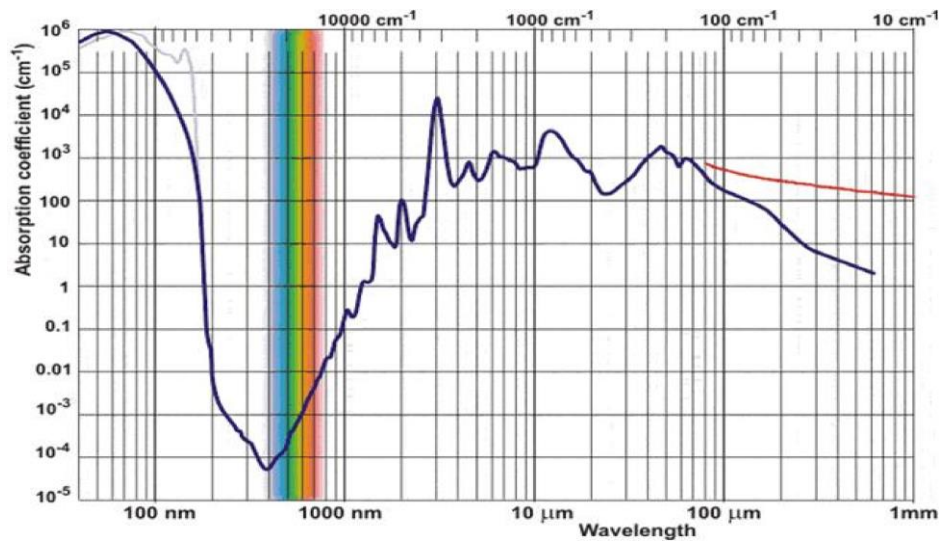


Fig.1 Transparent Window for Light Aquatic Attenuation [11, 12].

Absorption, scattering, and turbulence are the major elements influencing the UWOC [4].

2.1. Absorption and Scattering

In an underwater channel, light attenuation and directional shifts are caused by absorption and scattering, respectively [12]. The conversion of optical signals into thermal energy absorbed by suspended particles is known as absorption. Chlorophyll in phytoplankton absorbs colored dissolved organic matter (CDOM), whereas dissolved ions in water absorb chlorophyll; scattering causes photons to shift their orientation [4]. The total attenuation $c(\lambda)$ is represented in Eq.(1) [10]:

$$c(\lambda) = a(\lambda) + b(\lambda) \quad (1)$$

where $a(\lambda)$ represents the absorption coefficient, $b(\lambda)$ represents the scattering

coefficient, and (λ) represents the wavelength. Table 1 shows the typical values of $c(\lambda)$, $a(\lambda)$, and $b(\lambda)$ associated with four primary water types.

Table 1 The Attenuation for the Three Types of Water [13].

Water Type	$a(\lambda)(m^{-1})$	$b(\lambda)(m^{-1})$	$c(\lambda)(m^{-1})$
Clear water	0.114	0.037	0.151
Coastal water	0.179	0.220	0.399
Turbid Water	0.366	1.829	2.195

2.2. Turbulence in UWOC

Based on the beam scintillation index (σ_I^2) value, underwater turbulence can be classified into three channels: low, medium, and high (turbid water). The normalized variance of the laser irradiance is defined as the beam scintillation index. It is a metric for turbulence

intensity. The scintillation index is defined mathematically as [14]:

$$\sigma_I^2 = \frac{E[I^2]-E^2}{E^2[I]} \frac{E[h^2]}{E^2[h]} - 1 \quad (2)$$

where I_0 is the intensity for free fading, and $E[x]$ refers to the predictable value for the random variable x .

3.SYSTEM MODEL

Figure 2 shows the block diagram for the system model, which contains three parts. The first one is the transmitter side and receiver side. On the transmitter side is the source of the input message, the encoder (RS+CC), modulation (OOK), and several transmitter antennas, i.e., laser diodes. The second part includes the channel underwater. The last part represents the receiver side number of antenna use (photodetector), demodulation (OOK), decoding of (RS+CC), and detected message. A comparison with the input message is clear below, and the parameter used in the simulation is cleared in Table 2. The present work considers a laser source with a wavelength $\lambda = 470 \text{ nm}$ on the transmitter side and a photodetector on the receiver side, with a 30m separation between them. Each source is in the line-of-sight FOV from the receiver, with the Divergence Angle (DA) and 5cm-distance between each neighboring transmitter-receiver, as in [2]. A MIMO array was considered.

Table 2 Simulation Parameters.

Parameters	Value
Wavelength operation	470 nm
Water type	clear
Attenuation	0.151m^{-1}
Electronic bandwidth	2GHZ
Load resistance of the detector	100 Ω
Noise variance σ^2	2.82×10^{-33}
Distance L	30m
Data rate	500Mbps
detector's responsively η	0.8(AW)
Variance of the Gaussian distributed σ_x^2	0.1647
Scintillation index σ_I^2	0.9328

The concatenated technique is a well-known error correction code (ECC) that employs two

components. The outer code (block code) and the inner code (convolution code) are concatenated to achieve a comparatively high coding gain compared to a single code. The benefit of using concatenated code is that it exploits the feature of the block code (reed Solomon code and convolution code) to overcome each other's drawbacks. The total code rate in the transmitter is the product of each code [15]. The RS encoder encodes the data bits after they have been divided into m -bit symbols. The RS encoder produces $(n-k)$ check symbols after receiving a block of k information symbols. To create an RS code word with n symbols, the check symbols were added to the information symbols. Following symbol interleaving, the output of the RS encoder was fed to a Convolutional encoder before being sent across the channel to the receiver. Using a Galois Field $GF(q = 2^6)$, RS-code $(63, 51)$ is represented as in [2]:

$t=6$ symbols error, it is equivalent to a binary 6-tuple.

The codeword polynomial's constituent symbols are each translated into a 6-tuple of binary bits. The generator polynomial is:

$$G(x) = (x - a)(x - a^2) \dots (x - a^{2^t-1})(x - a^{2^t}) \quad (3)$$

$$M(x) = m_0 + m_1x + m_2x^2 + \dots + m_{k-1}x^{k-1} \quad (4)$$

where $m(x)$ is the input signal. The codeword polynomial is:

$$C(x) = m(x) \times g(x) \quad (5)$$

Then, by assuming the same interleaving that was used in [16], this interleaving structure will be as an array with a depth w of Reed Solomon code, so that the Code word array be as:

- Code word 1 $C_{11}, C_{21}, \dots, C_{n1}$
- Code word 2 $C_{12}, C_{22}, \dots, C_{n2}$
- Code word w $C_{1w}, C_{2w}, \dots, C_{nw}$

The input symbols to the Convolutional encoder in the following way:

$$C_{11}, C_{12}, C_{1w}, C_{21}, C_{22}, C_{2w}, \dots, C_{n1}, C_{n2}, \dots, C_{nw}$$

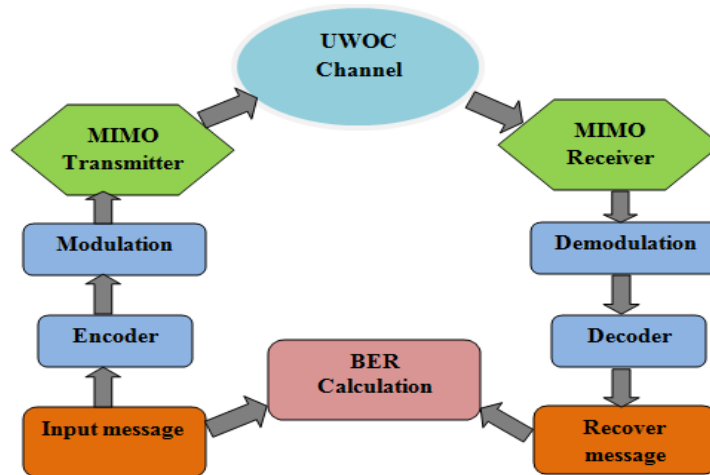


Fig.2 Block Diagram for the System Model.

Assume the structure of the Convolution code as in Fig. 3 [17] with the bite rate of 1/3 bit per second. So, the output matrix of the Convolution encoder will be:

$$OP(D) = [OP1(D) \ OP2(D) \ OP3(D)] \quad (6)$$

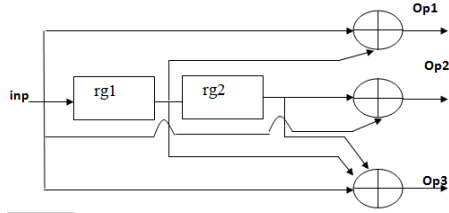


Fig.3 A Rate 1/3 Linear Convolutional Encoder [17].

In the OOK modulation system, the modulation symbols will be the binary bit zero (o) linked with (o) w of the transmitted optical power, which has an amplitude value (A) equal to zero. Also, the binary bit (1) is linked with the Pt, the optical power transmitted that equals.

$$A = (PtTb/N) \quad (7)$$

where N represents the number of optical sources. The two main noise sources in optical wireless communication systems are thermal noise on the receiver side and photon noise. The discreteness of photon arrivals, mostly caused by background light sources, results in photon noise. Even though received background light can be reduced through optical filtering, shot noise still develops in even a well-designed photodetector. The transmitted optical signal insignificantly contributes to this shot noise since the background light output is typically greater than the transmitted signal [19, 20, and 21]. All the noise was ignored, assuming that thermal noise was the only source of noise variation compared to other noise [2]. A Monte Carlo simulation technique was employed to model the channel impulse response. This UWOC channel's weak turbulence-free impulse response $h_{o,ij}(t)$ uses the lognormal probability density function (PDF), irradiance fluctuation, or multiplicative fading coefficient due to underwater weak turbulence \hat{h}_{ij} as in [2, 22].

$$F_{\hat{h}_{ij}} = \frac{1}{2\hat{h}_{ij} \sqrt{2\pi\sigma_{X_{ij}}^2}} \exp\left(-\frac{(\ln\hat{h}_{ij}-2\mu_{X_{ij}})^2}{8\sigma_{X_{ij}}^2}\right) \quad (8)$$

where $\mu_{X_{ij}}$ and $\sigma_{X_{ij}}^2$ represent the mean and variance of the Gaussian distributed log-amplitude factor $X_{ij} = -\frac{1}{2} \ln(\hat{h}_{ij})$, respectively. The probability density function (PDF) can be obtained by assuming $E[\hat{h}_{ij}] = 1$, which implies $\mu_{X_{ij}} = -\sigma_{X_{ij}}^2$, so that the impulse response between any *ith* transmitter and any receiver *jth* can be represented as $h_{ij} = \hat{h}_{ij}h_{o,ij}(t)$, Received optical signal from T_i to the R_j receivers as in [2, 23]:

$$Y_j = S(t) * h_{ij}(t) + n(t) \quad (9)$$

where $n(t)$ represents the additive white Gaussian Noise (AWGN) having zero mean and variance σ^2 in the receiver area after OOK

demodulation first decoding by inner decoder Convolution decoder, and use the hard decision Viterbi decoding [18] because it is easy, less complex, and cheaper than soft decision, where the input sequences to CC decoder is:

$$R = E + N \quad (10)$$

where E is the codeword transmitted, and N is the noise sample. A row and column symbol deinterleaver is used in the deinterleaving procedure. Deinterleaving reassembles the Viterbi decoded symbol sequence into an RS code matrix, and the decoding process was applied to all RS codewords, as in [24]. The reception vector $re(x) = re(0) + re(1)x + re(2)x^2 + \dots + re(n-1)x^{n-1}$; where $re(i)$ represents the extracted *ith* symbol, $i = 0, 1, \dots, n-1$, then processed to find the error positions, error values, and Forney's approach, which calculates the error values. Berlekamp-Massey and Chien [20] searched for algorithms to pinpoint where the channel caused problems. The estimated transmitted codeword was then calculated using the formula: $\hat{c}(x) = re(x) - er(x)$, i.e., $er(x) = \sum_{i=0}^{n-1} e_i x^i$, where e_i is the *ith* error magnitude given by Forney's method, and x^i is the *ith* error location found by Berlekamp-Massey and Chien search algorithms, as in [2, 21].

4.SIMULATION RESULTS

The present work used a pseudo-random generator. The UWOC channel transmitted the irradiance that the laser sources created. The detector processed the irradiance values received to estimate the conveyed data bit. Then, it estimated the bit error rate for the MIMO configuration so that $BER = \sum_i^l \frac{d_i \oplus \hat{d}_i}{l}$, where d_i/l are the transmitting bits, and \hat{d}_i is the data bits that transfer through the system. Fig.4 shows the BER estimation using a single input source and a single output receiver. The power transmitted at BER 10^{-5} was 37.50db. Figs. 4 and 5 show the transmit power gain per bit (db). For MISO, SIMO configuration for 2x1 and 1x5 without coding, the power transmitter performances were 11.40db and 21.20db, respectively, as increasing the transmitters source compared to SISO uncoded at BER 10^{-5} . Also, an improvement was noticed in power transmitted when using MIMO configuration 2x5 26.50db, as shown in Table 3. Fig. 6 shows that using the coding channel (Reed Solomon with convolution code) improved the transmitting power gain with respect to uncoded SISO configuration at BER 10^{-5} as the number of transmitters and receivers (2x1, 1x5) increased, i.e., 20.50db and 30.75db, respectively, as shown in Table 4. As shown in Fig. 7, using channel coding and MIMO structure 2x5, the transmitter power gain improved compared with the uncoded SISO at 10^{-5} , i.e., the gain Power approximated 33.60db, as shown in Table 4.

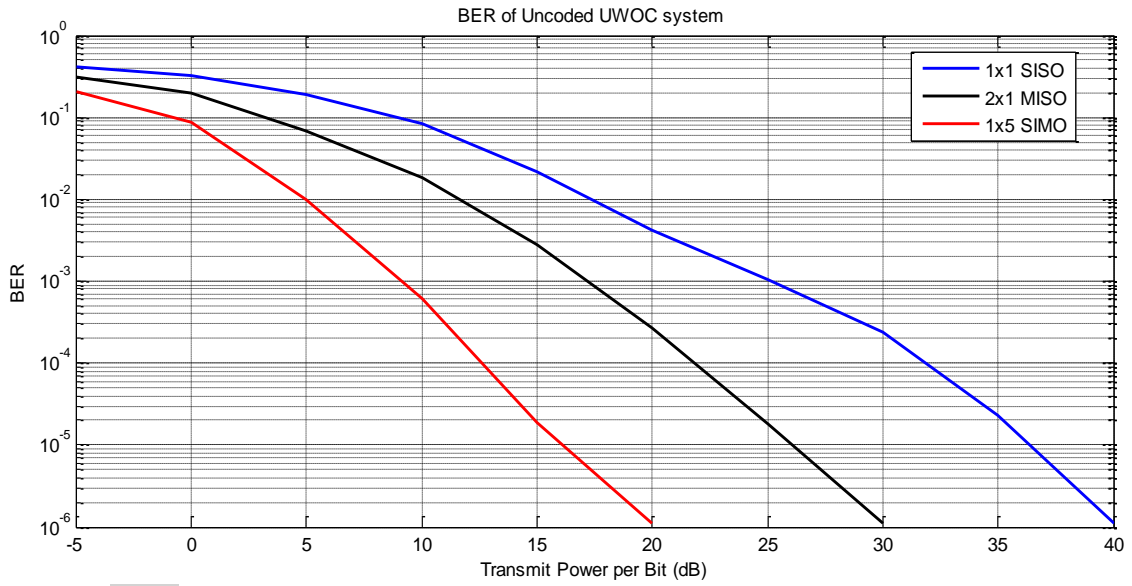


Fig.4 BER vs. Power Transmits per bit (db) Uncoded SISO, MISO, and SIMO.

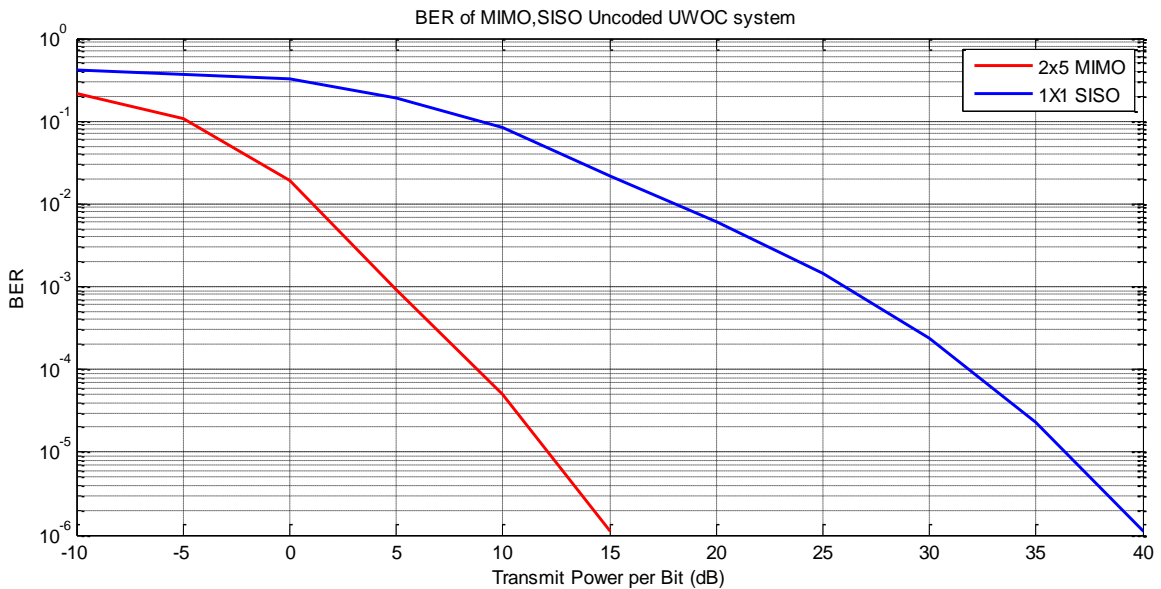


Fig.5 BER vs. Power Transmits per bit (db) Uncoded MIMO.

Table 3 Power Gain with Respect to Uncoded SISO.

MISO, MIMO Uncoded	Transmit power (dB) at BER of 10^{-5}	Power gain (dB) upon with uncoded SISO
1X1	37.50	-
2X1	18.90	11.40
1X5	16.30	21.20
2X 5	11.00	26.50

Table 4 Power Gain of Channel Coding with Respect to Uncoded SISO.

MIS, MIMO coded	Transmit power (Db) at BER of 10^{-5}	Power gain (Db) upon with respect uncoded SISO	Power gain (Db) upon with respect uncoded SISO [2]
1X1	22.50	15	27.50
2X1	17	20.50	18.90
1X5	6.75	30.75	9.90
2X 5	3.90	33.60	5.75

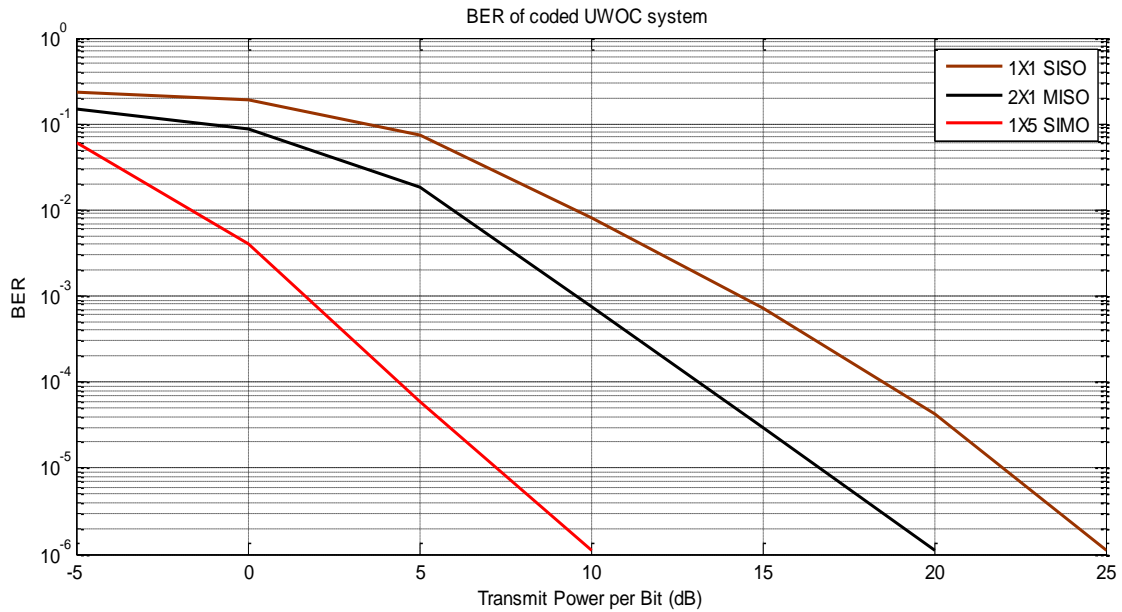


Fig.6 BER vs. Power Transmits per bit (db) Coded MISO, SIMO.

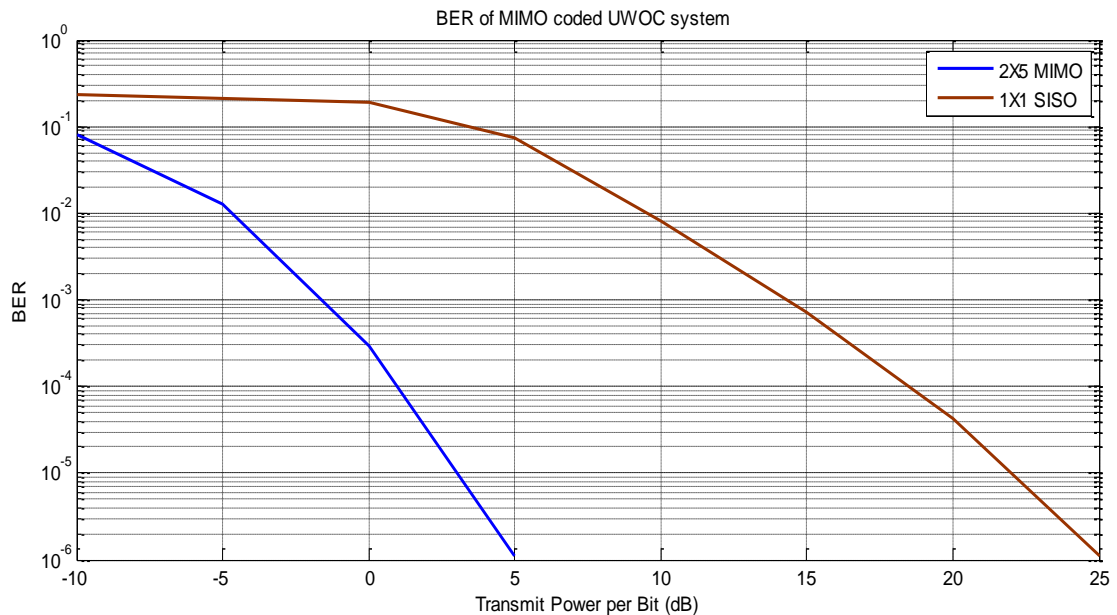


Fig.7 BER vs. Power Transmits per bit (db) Coded MIMO.

5. CONCLUSIONS

In this work, the Underwater Wireless Optical Communication channel was simulated using the concatenated code RS and CC, using different structures of MIMO, and considering the main losses that happened for light propagation in water attenuation and weak turbulence. The performance improved for the power transmitter compared with SISO uncoded at BER 10^{-5} . Therefore, it was concluded that using concatenated code for channels with different MIMO diversity 2x1, 1x5, and 2x5 improved the power gain by about 20.50, 30.75, and 33.60, respectively, which implies a consumption decrease in power transmitting. To enable IoUT applications; including inter-submarine communication,

boat dock communication, and communication between devices recording oceanic characteristics and combining devices; the suggested coded multi-input multioutput schemes can be used to implement Underwater Wireless Optical Communication systems. The challenge for future work is increasing the distance between the devices to increase the attenuation and the Intersymbol interference. Orthogonal frequency division multiplexing (OFDM) is recommended to increase data rate and link range and decrease intersymbol interference.

NOMENCLATURE

MIMO	multiple input-multiple output
MISO	multiple input-single output
SISO	single input-single output
SIMO	single input- multiple output
α	attenuation
λ	Wavelength
$S(t)$	transmitted signal
Y_j	receive signal
h_{ij}	impulse response between transmitter and receiver
n	noise signal

REFERENCES

- [1] Rizvi HH, Enam RN, Khan SA, Akram J. **A Survey on Internet of Underwater Things: Perspective on Protocol Design for Routing.** In *2020 Global Conference on Wireless and Optical Technologies (GCWOT) 2020*; Malaga, Spain. IEEE: 1-8.
- [2] Ramavath PN, Udupi SA, Krishnan P. **High-Speed and Reliable Underwater Wireless Optical Communication System Using Multiple-Input Multiple-Output and Channel Coding Techniques for IoUT Applications.** *Optics Communications* 2020; **461**:125229, (1-8).
- [3] Jamali MV, Salehi JA, Akhoundi F. **Performance Studies of Underwater Wireless Optical Communication Systems with Spatial Diversity: MIMO Scheme.** *IEEE Transactions on Communications* 2016; **65**(3):1176-1192.
- [4] Kaushal H, Kaddoum G. **Underwater Optical Wireless Communication.** *IEEE Access* 2016; **4**:1518-1547.
- [5] Zhu S, Chen X, Liu X, Zhang G, Tian P. **Recent Progress in and Perspectives of Underwater Wireless Optical Communication.** *Progress in Quantum Electronics* 2020; **73**:100274.
- [6] Tang S, Zhang X, Dong Y. **Temporal Statistics of Irradiance in Moving Turbulent Ocean.** In *2013 MTS/IEEE OCEANS-Bergen 2013*; Bergen, Norway. IEEE: 1-4.
- [7] Shen D, Tao L, Yu J, Ye P, Sheng Z, Zhou L, Shi M, Mei S, Wan X, Lian X, Liu X. **Disruptive Technology of Building Internet of Underwater Things: Laser-based Underwater Solid-State Lighting.** *5th IEEE Electron Devices Technology & Manufacturing Conference (EDTM) 2021*; Chengdu, China. IEEE: 1-3.
- [8] Mattoussi F, Khalighi MA, Bourennane S. **Improving the Performance of Underwater Wireless Optical Communication Links by Channel Coding.** *Applied Optics* 2018; **57**(9): 2115-2120.
- [9] Saaber S, Hassib MD, Jameel ZN. **A Review: Error Correcting Codes for Efficient Underwater Optical Communication MIMO System.** *Iraqi International Conference on Communication and Information Technologies (IICCIT) 2022*; Basrah, Iraq. IEEE: 13-19.
- [10] Chen R, Du J, Wang Y, Fei C, Zhang T, Tian J, Zhang G, Hong X, He S. **Experimental Demonstration of Real-Time Optical DFT-S DMT Signal Transmission for a Blue-LED-based UWOC System Using Spatial Diversity Reception.** *Applied Optics* 2023; **62**(3):541-551.
- [11] Azzawi HM, Ali AH, Gitaffa SA, Kadhim SA, Azawi HA. **Performance Evaluation of Dual Polarization Coherent Detection Optical for Next Generation of UWOC Systems.** *International Conference on Computer Science and Software Engineering (CSASE) 2020*; Duhok, Iraq. IEEE: 117-122.
- [12] Zeng Z, Fu S, Zhang H, Dong Y, Cheng J. **A Survey of Underwater Optical Wireless Communications.** *IEEE Communications Surveys & Tutorials* 2016; **19**(1):204-238.
- [13] Gussen CM, Diniz PS, Campos ML, Martins WA, Costa FM, Gois JN. **A Survey of Underwater Wireless Communication Technologies.** *Journal of Communication and Information Systems* 2016; **31**(1):242-255.
- [14] Sharifzadeh M, Ahmadirad M. **Performance Analysis of Underwater Wireless Optical Communication Systems Over a Wide Range of Optical Turbulence.** *Optics Communications* 2018; **427**:609-616.
- [15] Hassib MD, Abdullah M, Ismail M, Nordin R, MT I. **Improved Concatenated (RS-CC) for OFDM Systems.** *IEICE Electronics Express* 2012; **9**(6):538-543.
- [16] Aitsab O, Pyndiah R. **Performance of Concatenated Reed-Solomon/Convolutional Codes with Iterative Decoding.** In *GLOBECOM 97. IEEE Global Telecommunications Conference. Conference Record 1997*; Phoenix, AZ, USA. IEEE: Vol. 2, 934-938.
- [17] Rao KD. **Channel Coding Techniques for Wireless Communications.** Berlin, Germany: Springer India; 2015.
- [18] Sonawane S, Baste VS. **Implementation of RS-CC Encoder and Decoder using MATLAB.** *International Journal*

- of Science Technology and Engineering* 2019; **5**:22-30.
- [19] Fernando N, Hong Y, Viterbo E. **Flip-OFDM for Optical Wireless Communications**. IEEE Information Theory Workshop 2011; (pp. 5-9). IEEE.
- [20] Kahn JM, Barry JR. **Wireless Infrared Communications**. *Proceedings of the IEEE* 1997; **85**(2):265-298.
- [21] Carruthers JB, Kahn JM. **Modeling of Nondirected Wireless Infrared Channels**. *IEEE Transactions on Communications* 1997; **45**(10):1260-1268.
- [22] Jamali MV, Salehi JA. **On the BER of Multiple-Input Multiple-Output Underwater Wireless Optical Communication Systems**. *4th International Workshop on Optical Wireless Communications (IWOW) 2015*; Istanbul, Turkey. IEEE: 26-30.
- [23] Nawaf SF. **Channel Capacity Improvement of MIMO Communication Systems using Different Techniques**. *Tikrit Journal of Engineering Sciences* 2018; **25**(1):36-41.
- [24] Aitsab O, Pyndiah R. **Performance of Concatenated Reed-Solomon/Convolutional Codes with Iterative Decoding**. *IEEE Global Telecommunications Conference. Conference Record 1997*; Phoenix, AZ, USA. IEEE: 934-938.